Proc. Natl. Acad. Sci. USA
Vol. 89, pp. 5142–5146, June 1992
Biophysics

A model of the molten globule state from molecular dynamics simulations

(protein unfolding/solution simulations/protein folding intermediates)

VALERIE DAGGETT AND MICHAEL LEVITT

Beckman Laboratories for Structural Biology, Department of Cell Biology, Stanford University School of Medicine, Stanford, CA 94305-5400

Communicated by Robert L. Baldwin, March 9, 1992

ABSTRACT **It is generally accepted that a protein's primary sequence determines its three-dimensional structure. It has proved difficult, however, to obtain detailed structural information about the actual protein folding process and intermediate states. We present the results of molecular dynamics simulations of the unfolding of reduced bovine pancreatic trypsin inhibitor. The resulting partially "denatured" state was compact but expanded relative to the native state (11–25%); the expansion was not caused by an influx of water molecules. The structures were mobile, with overall secondary structure contents comparable to those of the native protein. The protein experienced relatively local unfolding, with the largest changes in the structure occurring in the loop regions. A hydrophobic core was maintained although packing of the side chains was compromised. The properties displayed in the simulation are consistent with unfolding to a molten globule state. Our simulations provide an in-depth view of this state and details of water–protein interactions that cannot yet be obtained experimentally.**

A protein must assume a stable and precisely ordered conformation to perform its biological function properly. Although much is known about these conformations and their synthesis, little is known about the detailed structures and dynamic transitions that occur during protein folding. Determination of the structural characteristics of partially folded intermediate states are crucial for understanding the mechanism of folding. Unfortunately, the cooperative nature of folding results in only minute amounts of these intermediates at equilibrium. So, instead, kinetic means have been used to characterize transiently populated intermediates (1–3). However, it has been shown that a few proteins adopt stable, partially folded equilibrium intermediates under unfolding conditions (4). There is some evidence that these intermediates, termed "molten globules," also occur along the kinetic pathway (ref. 4 and references therein). However, the molecular details of even the equilibrium folding intermediates remain difficult to characterize experimentally.

Here we present the results of molecular dynamics (MD) simulations of protein unfolding and the resulting partially unfolded structures. The approach of studying unfolding instead of folding has computational advantages, because simulations proceed from a well-defined starting structure. In principle, MD is capable of providing detailed information about unfolding and the resulting unfolded state that cannot be obtained experimentally. This method has yielded realistic representations of a native protein in water (5, 6) and has been useful in understanding the nature of less-structured peptides (7–9) and the unfolding–folding transitions that they undergo (7, 10, 11). The studies presented here focus on bovine pancreatic trypsin inhibitor (BPTI) because it is a small, well-characterized protein (ref. 12 and references therein).

The unfolding of BPTI from its native conformation, but with reduced disulfide bonds, was achieved by disrupting the structure with high temperature. While it is not known how fast proteins unfold, it is usually thought to be in the millisecond range, or faster. This time scale is not accessible by MD simulations; the simulations presented here require ≈2 central processing unit (CPU) hr/ps. Hence, we chose to use high temperature as a means of accelerating the process. Raising the temperature has a small effect on the velocities (atoms at 498 K move ≈30% faster than at 298 K), but activated processes involving jumping over energy barriers will be accelerated by ≈5 orders of magnitude. Five MD simulations (lasting up to 550 ps) were performed: native BPTI at 298 K and 423 K; reduced BPTI at 298 K, 423 K, and 498 K. All simulations were carried out in a bath of water molecules with mobile counterions. Here we describe the partially unfolded conformations generated with MD; the actual unfolding process will be described elsewhere.

METHODS

Preparation of the Protein–Solvent Models. The x-ray crystal structure of BPTI (4PTI; ref. 13) was used as the starting point for the various simulations. All minimization and MD procedures were performed with the program ENCAD (14). All atoms were explicitly present during the simulations, and the potential energy function and associated parameters are based on those described earlier (15, 16), except for the parameters for chloride ($R^* = 2.35$ Å; $\varepsilon^* = 0.10$ kcal/mol); the full details of the potential will be presented elsewhere. The chloride parameters were chosen to give experimentally reasonable distances between the ions and water during MD [Cl⁻···O distance of 2.9–3.4 Å in the simulation and 3.1–3.4 Å experimentally (17)]. All of the charged residues carried full charges.

A variety of procedures were performed to prepare the BPTI systems, at different temperatures with or without disulfide bonds, for MD. In each case, where energy minimization was employed, 2000 cycles were executed. First, the crystal structure of BPTI was minimized. Then, water molecules were added to fill a rectangular box extending at least 8 Å from any protein atom, resulting in the addition of 2515 water molecules. The volume of the box was adjusted to give the experimentally observed density for water at the temperature of interest: 0.997 g/ml at 298 K, 0.916 at 423 K, and 0.829 at 498 K (18). Six chloride ions were then added at random, replacing 6 water molecules to yield an electrically neutral system. The water molecules were then minimized, MD of water was performed for 2000 steps, and minimization of water was again performed. The protein was then minimized, followed by minimization of the full system.

Secondary structure fragments of BPTI were also simulated. The isolated C-terminal α-helix (residues 47–56) and

The publication costs of this article were defrayed in part by page charge payment. This article must therefore be hereby marked "*advertisement*" in accordance with 18 U.S.C. §1734 solely to indicate this fact.

Abbreviations: BPTI, bovine pancreatic trypsin inhibitor; MD, molecular dynamics.

the central β-sheet (residues 16–36) were excised from minimized BPTI. The termini were blocked (acetylated at the N terminus and amidated at the C terminus). Zero and 3 chloride ions and 708 and 1508 water molecules were added to the α-helix and β-sheet, respectively. The preparatory steps described above were employed. Two simulations of each model were performed, at 423 and 498 K.

Details of MD Simulations. Classical MD was performed at constant volume, employing periodic boundary conditions. The minimized systems were brought to the target temperature by scaling the velocities. After the desired temperature was reached, no further adjustment of the velocities was necessary. The simulations proceeded for up to 550 ps for each full protein system and 200 ps for the fragments. An 8-Å nonbonded list was employed, the nonbonded list was updated every 2–5 cycles, and 2-fs time steps were used. The energy was well conserved; there was a 0.5–0.8% drift in the total energy. At 498 K, however, the system became unstable after 284 ps and further structures were not considered for analysis. Structures were saved every 0.2 ps for analysis.

RESULTS

Characteristics of the partially unfolded state were as follows.

Shape and Size. In our simulations, the radius of gyration was 4–9% greater in reduced BPTI at high temperature than in the control simulations (native BPTI at 298 and 423 K and reduced BPTI at 298 K) (Table 1). The average volume of reduced BPTI increased by 11–25% with increasing temperature (Table 1); this was not just a temperature-induced phenomenon, as the volume of reduced BPTI at 423 K was greater than that of the oxidized form. The water-accessible surface area also increased in reduced BPTI at high temperature, by 19–27% (Table 1). Hence, reduced BPTI at high temperature remained compact but was larger than the controls (Fig. 1).

Internal Motion. Reduced BPTI exhibited considerably more motion at high temperature than in the control simulations, with the average rms displacement of the α carbons from their positions in the crystal structure increasing from 1.7 Å to as much as 5.1 Å (Table 1). The disulfide bonds strongly constrained the protein at high temperature; the C^α rms deviation was ≈50% higher in the reduced protein at 423 K than in the oxidized form. Surprisingly, at 498 K many α-carbons had rms displacements over 8 Å from their starting positions (Fig. 2) and maximum displacements of over 14 Å (residue 58 showed the largest deviation, 18.8 Å). The comparison of our simulations to a single crystal structure may accentuate the extent of motion (22), especially for native BPTI at low temperature. Kossiakoff *et al.* (22) have compared the variability of five different BPTI crystal structures, each in a different packing environment, and found that particular regions of the sequence are structurally variable. In particular, these regions correspond to the peaks in Fig. 2.

The unfolded structures of reduced BPTI at high temperature did not adopt a single conformation. Instead, the fluctuations of the α-carbons about their mean positions during the last 150 ps of the simulation indicate that there was significant motion in these structures and that various conformations were sampled even though the overall C^α rms deviations from the crystal structure had stabilized. We stress that the conformation depicted in Fig. 1 is a representative structure and should not be considered *the* structure of the molten globule state (Table 1).

The fluctuations in the main-chain dihedral angles φ and ψ increased ≈70% at high temperature (Table 1). The fluctuations of the side-chain dihedral angles χ_1 and χ_2 were also considerably greater in the high temperature simulations (by 120–160%; see Table 1). The simulation of oxidized BPTI at 423 K demonstrates that the increase in internal motion is not just a result of increasing the temperature, as all of the properties discussed were lower in the oxidized than in the reduced form. The largest fluctuations, at 498 K, were still much smaller than would be expected for freely rotating side chains (≈45° versus ≈90°).

Table 1. Overall average properties of BPTI as a function of temperature and oxidation state of the disulfide bonds

Property	Oxidized		Reduced		
	298 K	423 K	298 K	423 K	498 K
Time, ps	550	550	550	550	284
R_g,[a] Å	11.6	11.7	11.9	12.1	12.6
ΔV,[b] %	−2	0	5	11	25
ΔA,[c] %	6	13	11	19	27
C^αrmsd,[d] Å	1.7	2.7	2.5	3.9	5.1
C^αfluc,[d] Å	0.7	1.1	0.7	2.1	2.4
$\Delta\phi$,[e] degrees	15	21	14	24	25
$\Delta\psi$,[e] degrees	15	21	15	24	28
$\Delta\chi_1$,[e] degrees	16	31	22	39	45
$\Delta\chi_2$,[e] degrees	19	33	25	38	44
Total 3° intact,[f] %	90	83	84	76	69
Native 3° intact,[f] %	79	72	71	55	53
Total 3° non-native,[f] %	13	13	15	30	26
Ring flips,[g] no.	0	4	0	16	15
α-Helix,[h] %	28	28	28	27	22
β structure,[h] %	43	42	43	34	45
Native α HB,[i] %	54	52	52	47	40
Native β HB,[i] %	66	77	62	31	53
α HB,[i] no.	6	8	6	7	6
β HB,[i] no.	10	11	8	5	8
Buried waters,[j] no.	7	5	6	8	8
NHCO···H_2O contacts,[k] no.	114	92	109	108	95
NHCO···H_2O HB,[k] no.	62	34	60	41	35

All properties were averaged over the entire simulation, considering all structures collected for analysis (2750 structures for 550 ps and 1420 for 284 ps), unless other averaging intervals are specifically mentioned.

[a]Computation of the radius of gyration has been described (5). The value for the starting structure is 11.7. SD = 0.1–0.2 Å.

[b]The volume was calculated from R_g by assuming that the protein is spherical. Here, $\Delta V = 100 \times (\langle V \rangle - V_0)/V_0$ where V_0 = 6709 Å^3 and is the volume of native BPTI prior to MD and ⟨⟩ denotes an ensemble average. SD ≈ 2%.

[c]Percent change in the solvent-accessible surface area (19), A_0 = 4094 Å^2. SD was 3% at 298 K and ≈6% at high temperature.

[d]C^α rmsd is the average root-mean-square (rms) displacement of the α carbons from the crystal structure after equilibration (e.g., 50–550 ps). To eliminate Brownian motion, rmsd is calculated after optimum superposition of the protein coordinates (20). C^α fluctuation is the rms displacement from the mean structure over the final 150 ps of the simulations.

[e]All the rms fluctuations in dihedral angles were averaged over both time and all relevant dihedral angles (57 main-chain dihedrals, 42 χ_1 and 34 χ_2 angles).

[f]Percentage of native, non-native, and total tertiary contacts (≤4.5 Å) between non-neighboring residue pairs; there are 224 contacts in the crystal structure.

[g]Total number of ring flips (180° rotation about χ_2) that occurred during the simulations.

[h]α-Helix content was defined as having both φ and ψ for a particular residue within ≈50° of the ideal values for α-helical and β conformations averaged over all time and all residues (8, 10, 11).

[i]Percentage of intact native hydrogen bonds (≤2.6 Å) was averaged over time and the particular hydrogen bonds. There were 9 within α-helices and 10 between the β-strands in the crystal structure. Total number of hydrogen bonds includes those within α-helices or between β-strands, including non-native interactions, that were present ≥20% of the simulation time.

[j]Average number of water molecules that were not within contact of any bulk waters. Average SD was 4.8.

[k]Average number of peptide bond–water contacts (distance ≤ 2.6 Å); SD was 7.5. Peptide bond–water hydrogen bonds (HB) have the added angular constraint, 135° ≤ θ ≤ 180°; average SD was 6.7.

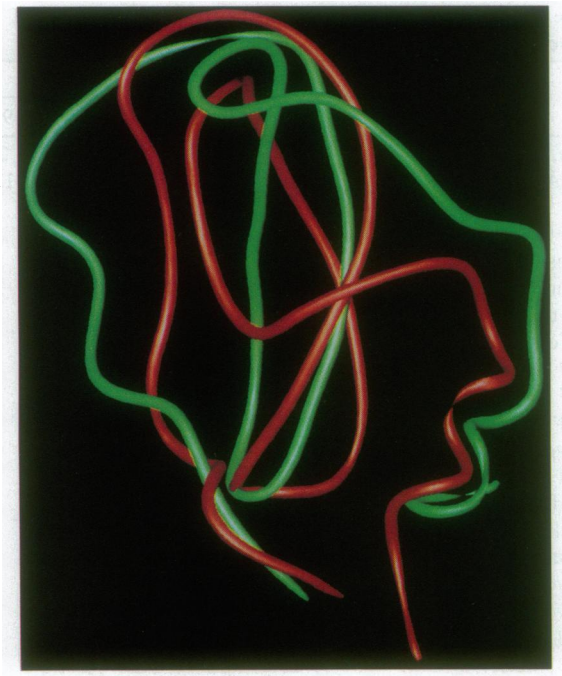

FIG. 1. Ribbon drawings [generated with MIDAS (21)] of main-chain atoms of the average structure of reduced BPTI at 498 K (green; 150–200 ps) superimposed on the x-ray structure (red).

Internal Packing. A variety of properties were monitored in an attempt to determine the changes in internal packing within the models. The packing density of reduced BPTI at high temperature necessarily decreased since the protein volume increased, yielding a lower number of total tertiary contacts between non-neighboring residues (Table 1). The number of native contacts decreased appreciably in reduced BPTI at high temperature (Table 1). The number of non-native tertiary contacts increased, however, in the unfolded models (Table 1).

As a result of the decreased packing density, the rings of at least six of the eight aromatic residues in reduced BPTI flipped (180° rotation about χ_2) at least once in the simulations of reduced BPTI at 423 and 498 K (Table 1). Only two of the aromatic residues flipped in the simulation of oxidized BPTI at 423 K. The demonstration of ring flips is significant not only because it reflects internal changes in packing and motion, but also because ring flips were not observed previously in free MD simulations (ref. 5; see ref. 23 for review).

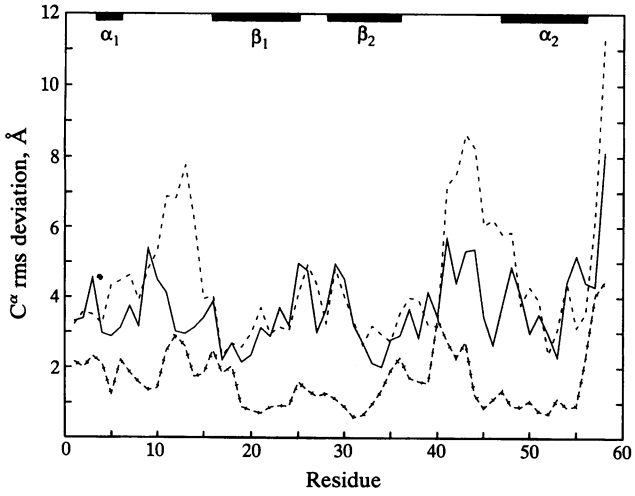

FIG. 2. C^{α} rms displacements from the crystal structure as a function of temperature averaged over the entire simulations for native BPTI at 298 K (crossed line) and for reduced BPTI at 423 K (solid line) and 498 K (dashed line).

About half (40–50%) of the increase in solvent-accessible surface area at high temperature was due to the exposure of nonpolar residues. The normal distribution of aromatic residues in BPTI was drastically altered in the reduced structure at 498 K (Fig. 3). The reduced structure maintained something of a hydrophobic core consisting of two to four phenylalanine residues (depending on time) with Phe-22 and -33 being most important, while the four tyrosine residues were at, or near, the surface of the molecule.

Secondary Structure. The percentage of residues adopting α-helical or β structure in the simulations was 61–71%, and this degree of structure was essentially independent of temperature and the state of the disulfide bonds (Table 1). At 498 K the average percentage of helix was lower than in native BPTI, whereas the amount of β structure increased slightly (Table 1; Fig. 1). The existence of hydrogen bonds was not necessary for secondary structure formation, nor did their presence ensure the formation of secondary structure, although in general the two phenomena were correlated (Table 1). The molecules experienced relatively local unfolding, with the largest disruptions to the structure occurring in the loop regions (Figs. 1 and 2). Further, the very mobile regions at high temperature also exhibited increased motion in the native structure at low temperature.

To determine the inherent stability of the secondary structure at high temperature, we performed separate short simulations (200 ps) of isolated fragments of the protein: the C-terminal helix and the central β-sheet. The isolated α-helix retained an average of 65% and 6% helix at 423 and 498 K, respectively [structure was defined by ϕ, ψ angles (11)], while the helix content during the same period of time in reduced BPTI was 77% and 65% at 423 and 498 K, respectively. The β-sheet contained 18% and 58% β structure in reduced BPTI at 423 and 498 K, respectively. The β content was 73% and 67% at these same temperatures in the simulations of the isolated β-sheet. The average secondary structure values fluctuated greatly with time, by 9–20%.

Water–Protein Interactions. The average number of buried water molecules was roughly independent of temperature and the oxidation state of the disulfides (Table 1). Therefore, the larger dimensions of the partially unfolded state cannot be explained by the burial of water molecules. The number of peptide bond–water contacts dropped with temperature. The number of contacts was lower in oxidized than in reduced BPTI at high temperature due to the increased exposure in the reduced form. The number of specific main chain–water hydrogen bonds decreased significantly, by 30–40%, at high temperatures (Table 1), with less hydrogen bonds in oxidized BPTI at 423 K than in the reduced form. Hence, it appears that the intramolecular hydrogen bonds in the folded state are not completely compensated by hydrogen bonds with solvent in the unfolded state.

One of the unfortunate side effects of decreasing the water density to relieve excess pressure at high temperature is that as water–protein interactions decrease, these interactions are further diminished by the increase in the entropy of the waters. To control for these effects, we took the unfolded structure at 498 K and performed MD at 298 K (for 10 ps) with the density raised appropriately. Under these conditions the number of water–peptide bond contacts and hydrogen bonds increased to 118.3 (from 94.9) and 77.9 (from 34.7), respectively. Thus, the water–protein interactions, at low temperature, do increase in the unfolded protein relative to the native state.

Energetics. The electrostatic energy of reduced BPTI at high temperature immediately increased 11–18% compared to native protein. However, the van der Waals energy

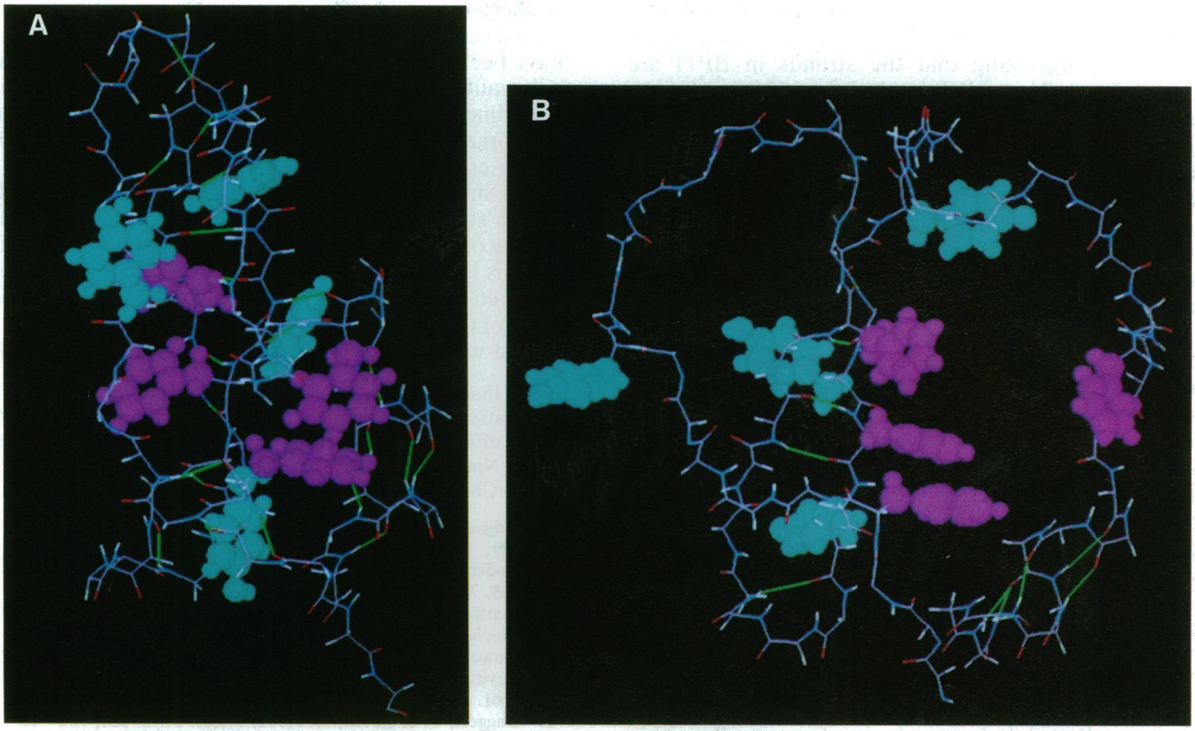

FIG. 3. Traces of the main-chain atoms of structures with the surfaces of the aromatic residues displayed, tyrosine in cyan and phenylalanine in magenta [generated with MACIMDAD, (39)]. Hydrogen bonds are shown in green. (*A*) Crystal structure of BPTI. (*B*) Reduced BPTI at 498 K (150–200 ps).

decreased 13–23% upon unfolding. Thus, at higher temperatures, entropy favors the less specific van der Waals interactions over the more specific electrostatic interactions.

DISCUSSION

The properties of the simulations of reduced BPTI at high temperature are consistent with unfolding to a molten globule state. The characteristics of the molten globule state are still debated; we use the following general definition: compact, mobile, partially structured conformations (24). It has been suggested that the molten globule state is a common intermediate in folding (ref. 25 and references therein), is populated in acid-denatured (26) and possibly in temperature-denatured proteins containing residual structure, and may also be involved in protein translocation (27). The molten globule state presumably accelerates attainment of the native conformation by allowing further folding and structural fine tuning to occur in a condensed volume. Detailed structural characterization of a molten globule is very difficult to obtain experimentally (28) because it is a poorly defined, mobile state. Experimentally, fully reduced BPTI demonstrates some properties of a molten globule (29). But unfortunately, little information is available for BPTI and we must rely on comparisons with the properties of other proteins. Fortunately, there is agreement between the various proteins on a variety of aspects.

Size and Motion. In our simulations, reduced BPTI at high temperature was compact but larger than oxidized BPTI under the same conditions. The expansion was not caused by solvent penetration. Experimentally, the molten globule state is dense and compact but slightly (10–25%) larger than the native conformation (in contrast, denatured proteins are ≈40% larger) (4, 25, 29). Both the main-chain and side-chain motion increased significantly in reduced BPTI at high temperature. The increased mobility of the molten globule state has been demonstrated by a variety of experimental methods (reviewed in ref. 25). Many α-carbons moved >14 Å in the simulation at 498 K, which is remarkable given that the structures remained compact. This result suggests that large-scale motion is possible within a collapsed state.

Packing. The unique, relatively rigid packing of side chains was compromised in reduced BPTI at high temperature. Diminished tertiary contacts and changes in the environment around aromatic residues have also been inferred from experiment (25). The solvent accessibility of the nonpolar and aromatic residues increased in reduced BPTI at high temperature, although a small hydrophobic core was maintained. Molten globules appear to have increased exposure and hydration of hydrophobic residues compared with the native state: they show increased binding of hydrophobic probes, their solubility in water decreases, they are more susceptible to aggregation, and the heat capacity increases (25). Although the degree of internalized water molecules in the unfolded models generated here was the same as in the control simulations, the increased exposure of the hydrophobic residues is consistent with the experimental results.

Secondary and Tertiary Structure. In the simulations, reduced BPTI retained native-like amounts of secondary structure at high temperature. Secondary structure contents of 60–200% of the native protein have been observed experimentally for molten globules (4, 25). Our models of reduced BPTI showed localized regions of structure, most of which were native-like, as has been observed for the molten globule state of α-lactalbumin (28), apomyoglobin (30), and ubiquitin (31).

Although the C-terminal α-helix was stable in isolation in the simulation, it was significantly more stable in the presence of the protein scaffolding, even when in a non-native conformation. The opposite was true of the central β-sheet; its structure was distorted by the surrounding protein, which diminished as the protein became more flexible. The C-terminal α-helix is indeed partially helical in solution at low temperature as measured by CD (32). Experimental work suggests that the isolated β-sheet is unstructured, however (33). The discrepancy between experiment and our simulations is probably due to the short simulation time and the fact that our simulation began with the folded form and made no

allowance for achieving that state. We have found that isolated β-strands are indeed unstable under these same conditions (11), suggesting that the strands in BPTI are mutually stabilizing. Nevertheless, these peptide simulations serve as controls for the simulations of the whole protein.

Unfolding in our simulations was relatively local in nature, occurring in turns and loops. Such localized unfolding has also been suggested from structural experimental studies of molten globules (24, 28, 30, 31). The β-sheet and α-helix of BPTI were mutually stabilizing. This folding unit represents the structurally important portion of the molecule, while the loop near the top of the molecule (Fig. 1) is involved in binding interactions with trypsin. In our simulations, the core of the molecule remained essentially intact, although altered, upon unfolding whereas the binding region was disrupted. Oas and Kim (34) have characterized a fragment of BPTI containing the C-terminal α-helix and most of the β-sheet, which is quasistable and contains native-like structure. In simulations of their fragment we have found secondary structure contents comparable to those in the simulation of reduced BPTI (data not presented), demonstrating the importance of particular interactions, or the folding units themselves, not only to the native state but also in the folding process, as suggested by Levitt and Chothia (35).

Time Scale of Unfolding. Unfolding is a difficult process to define for comparison of the time course of our simulations to experiment. Kinetic studies indicate that the process of folding to the molten globule state is very fast, usually within the experimental deadtime (millisecond scale, at best), and the attainment of the proper tertiary interactions from this state is slow (4). The latter step appears to be responsible for the cooperativity of folding, whereas the former is more gradual. These results suggest that the transition between the molten globule and native state may be more relevant to the folding process *in vivo* than the transition from the fully unfolded protein, and generally harsh conditions are necessary to completely unfold molten globules (25). The molten globule state can be attained not only during refolding but also during unfolding in some systems (25, 31).

We have little hope of reaching the millisecond time scale with detailed simulations, but these times are best viewed as lower limits. In fact, unfolding with chemical denaturants can be very fast relative to folding (36). This is possibly the case with temperature-catalyzed unfolding as well. Hence, the actual unfolding process may be much faster than milliseconds and experimental techniques probing different aspects of unfolding may give different results. For example, if the amount of secondary structure were used to monitor unfolding, our simulations would show almost no unfolding. In contrast, if the extent of tertiary contacts were used, then the simulations would show that unfolding was rapid. Therefore, the unfolding that we observed is in the range of a few picoseconds to the length of the simulation, 550 ps. The upper limit to the unfolding time would presumably increase further with longer simulations, since most of the changes in the properties after 100 ps were gradual.

We do have one straightforward measure of the time scale of the motion in the simulations, water diffusion. Diffusion is one of the few time-dependent properties that can be determined directly both experimentally and from simulations. The observed diffusion (0.24–1.72 $Å^2$/ps from 298 to 498 K) is lower but comparable in magnitude to the experimental values for pure water (0.25–3.45 $Å^2$/ps) (37). Water diffusion is known to decrease in biopolymer solutions (38).

Summary and Caveats. Although simulations to visualize unfolding can be useful in furthering our understanding of protein folding, it is difficult to definitively declare that we have indeed reached a molten globule state or that what we have modeled is physically relevant given that the simulation is short in the life of a protein. Our models do, however, reproduce all of the known features of molten globules and have been obtained during a free MD simulation without any adjustable parameters. Unfortunately, our comparisons to experiment are qualitative because of the limited structural experimental data available. It is gratifying that the nonnative conformations generated are consistent with experiment, since force fields are parameterized to reproduce the native state, not unfolded states. An important additional finding of our work is that the native protein is stable for >0.5 ns; this is the longest free simulation of a protein in solution reported thus far (most are 15–100 ps long) (6). The detailed steps of unfolding of BPTI to the molten globule state and the role of water in this process will be described elsewhere.

We thank I. D. Kuntz, P. A. Kollman, and R. L. Baldwin for many stimulating discussions and/or helpful comments. M. Hirshberg's efforts are also greatly appreciated. This work was supported by the National Institutes of Health (GM41455 to M.L.) and the Jane Coffin Childs Memorial Fund for Medical Research (to V.D.).

1. Udgaonkar, J. B. & Baldwin, R. L. (1988) *Nature (London)* **335**, 694–699.
2. Roder, H., Elove, G. A. & Englander, S. W. (1988) *Nature (London)* **335**, 700–704.
3. Matthews, C. R., Crisanti, M. M., Manz, J. T. & Gepner, G. L. (1983) *Biochemistry* **22**, 1445–1452.
4. Kuwajima, K. (1989) *Proteins Struct. Funct. Genet.* **6**, 87–103.
5. Levitt, M. & Sharon, R. (1988) *Proc. Natl. Acad. Sci. USA* **85**, 7557–7561.
6. Daggett, V. & Levitt, M. (1991) *Chem. Phys.* **158**, 501–512.
7. Daggett, V. (1990) Ph.D. thesis (Univ. of California, San Francisco).
8. Daggett, V., Kollman, P. A. & Kuntz, I. D. (1991) *Biopolymers* **31**, 285–304.
9. Tirado-Rives, J. & Jorgensen, W. L. (1991) *Biochemistry* **30**, 3864–3871.
10. Daggett, V., Kollman, P. A. & Kuntz, I. D. (1991) *Biopolymers* **31**, 1115–1134.
11. Daggett, V. & Levitt, M. (1992) *J. Mol. Biol.* **223**, 1121–1138.
12. Creighton, C. R. (1978) *Prog. Biophys. Mol. Biol.* **33**, 231–297.
13. Deisenhofer, J. & Steigemann, W. (1975) *Acta Crystallogr. Sect. B* **31**, 238–250.
14. Levitt, M. (1990) ENCAD—*Energy Calculations and Dynamics* (Stanford Univ., Stanford, CA; Yeda, Rehovot, Israel).
15. Levitt, M. (1983) *J. Mol. Biol.* **168**, 595–620.
16. Levitt, M. (1989) *Chem. Scr.* **29A**, 197–203.
17. Cummings, S., Enderby, J. E., Neilson, G. W., Newsome, J. R., Howe, R. A., Howells, W. S. & Soper, A. K. (1980) *Nature (London)* **287**, 714–716.
18. Kell, G. S. (1967) *J. Chem. Eng. Data* **12**, 66.
19. Lee, B. & Richards, F. M. (1971) *J. Mol. Biol.* **55**, 379–400.
20. Kabsch, W. (1976) *Acta Crystallogr. Sect. A* **32**, 922–923.
21. Jarvis, L., Huang, C., Ferrin, T. & Langridge, R. (1985) MIDAS (Univ. of California, San Francisco).
22. Kossiakoff, A. A., Randal, M., Guenot, J. & Eigenbrot, C. (1992) *Proteins Struct. Funct. Genet.* **12**, in press.
23. Karplus, M. & McCammon, J. A. (1983) *Annu. Rev. Biochem.* **53**, 263–300.
24. Dolgikh, D. A., Gilmanshin, R. I., Brazhnikov, E. V., Bychkova, V. E., Semisotnov, G. V., Venyaminov, S. Yu. & Ptitsyn, O. B. (1981) *FEBS Lett.* **136**, 311–315.
25. Ptitsyn, O. B. (1987) *J. Protein Chem.* **6**, 273–293.
26. Goto, Y., Calciano, L. J. & Fink, A. L. (1990) *Proc. Natl. Acad. Sci. USA* **87**, 573–577.
27. Bychkova, V. E., Pain, R. H. & Ptitsyn, O. B. (1988) *FEBS Lett.* **238**, 231–234.
28. Baum, J., Dobson, C. M., Evans, P. A. & Hanley, C. (1989) *Biochemistry* **28**, 7–13.
29. Amir, D. & Haas, E. (1988) *Biochemistry* **27**, 8889–8893.
30. Hughson, F., Wright, P. & Baldwin, R. L. (1990) *Science* **249**, 1544–1548.
31. Harding, M. M., Williams, D. H. & Woolfson, D. N. (1991) *Biochemistry* **30**, 3120–3128.
32. Goodman, E. M. & Kim, P. S. (1989) *Biochemistry* **28**, 4343–4347.
33. Goodman, E. M. & Kim, P. S. (1990) *Current Research in Protein Chemistry* (Academic, New York), pp. 301–308.
34. Oas, T. G. & Kim, P. S. (1988) *Nature (London)* **336**, 42–48.
35. Levitt, M. & Chothia, C. (1976) *Nature (London)* **261**, 552–558.
36. Beasty, A. M., Hurle, M. R., Manz, J. T., Stackhouse, T., Onuffer, J. J. & Matthews, C. R. (1986) *Biochemistry* **25**, 2965–2974.
37. Eisenberg, D. & Kauzmann, W. (1969) *Structure and Properties of Water* (Clarendon, Oxford, U.K.).
38. Cooke, R. & Kuntz, I. D. (1974) *Annu. Rev. Biophys. Bioeng.* **3**, 95–126.
39. Levitt, M. (1990) MACIMDAD (Stanford Univ., Molecular Applications Group, Stanford, CA; Yeda, Rehovot, Israel), Version 3.